This is the Accepted Manuscript version of a Published Work appeared in:

Journal of Physical Chemistry C, 2015, Volume 119, Pages 8191-8198

(DOI: 10.1021/acs.jpcc.5b00938)

Study of adenine and guanine oxidation mechanism by Surface-Enhanced Raman Spectroelectrochemistry.

D. Ibañez[1], A. Santidrian[2], A. Heras[1], M. Kalbáč[2], A. Colina[1].*

1. Department of Chemistry, Universidad de Burgos, Pza. Misael Bañuelos s/n, E-09001, Burgos, Spain.

2. J. Heyrovsky Institute of Physical Chemistry of the AS CR, v.v.i., Dolejskova 2155/3, CZ-182 23 Prague 8, Czech Republic

* Corresponding author: acolina@ubu.es, Tel: +34-947258817, Fax: +34-947258831.

Abstract

Metal nanoparticles are systems largely employed in surface-enhanced Raman spectroscopy (SERS). In particular, gold nanoparticles are one of the best substrates used in this field. In this work, the optimal conditions for gold nanoparticles electrodeposition on single-walled carbon nanotubes electrodes have been established to

obtain the best SERS response. Using this substrate and analyzing the changes of *in-situ* Raman spectra obtained at different potentials, we have been able to explain simultaneously the oxidation mechanism of purine bases, differentiating the oxidation intermediates, and their orientation during the different oxidation steps. Adenine orientation hardly changes during the whole oxidation; the molecule maintains a parallel configuration and only shows a slightly tilted orientation after the first oxidation step. On the other hand, guanine orientation changes completely during its oxidation. Initially, guanine is perpendicular respect to gold nanoparticles, changing its orientation after the first oxidation process when the molecule shows a slightly tilted orientation and it finishes parallel respect to the electrode surface after the second oxidation step.

Keywords

Surface-enhanced Raman scattering (SERS); spectroelectrochemistry; gold nanoparticles; adenine oxidation; guanine oxidation.

1. Introduction

Surface-enhanced Raman scattering (SERS) is a powerful analytical tool for sensitive and selective detection of different molecules adsorbed on metal nanostructured. Since this effect was observed in the 70s[1–3] it has been used in many fields[4–8] to study different systems and processes. However, one of the most important factors to take into account for SERS applications is the substrate. The development of different methods and procedures has allowed the improvement of SERS substrates from initially non-uniform substrates to the actual well-defined surface nanostructures in size, shape and interparticle spacing. The main properties that SERS substrates should show are high sensitivity, uniformity, good stability, surface purity and reproducibility.[9,10] Although it is quite complicated to obtain substrates with all these properties, metal (Au, Ag, Pd, Pt,…) nanoparticles (NPs) are systems largely employed in SERS.[11–15] In particular, gold deposition by plating processes provides SERS substrates with the long term stability and high enhanced factor.[16,17] Gold nanoparticles (AuNPs) are usually deposited onto different type of electrodes, making possible the study of electrochemical processes because of the higher SERS signal intensity related to the species involved in the electron transfer process.

Adenine and guanine are two important biologically active molecules, since they are essential components of nucleic acids. A strong interest to characterize DNA bases has grown during the last years, being particularly important for the study of the oxidation mechanism of these bases. This process is crucial since the oxidation of these bases can cause DNA damages and consequently cell damage or even death of cells. Purine and pyrimidine bases can be electrochemically oxidized.[18–21] In particular, adenine and guanine are oxidized at much lower positive potentials than thymine and cytosine. The analysis of Raman spectral data is very complex because of the presence of different

oxidation intermediates and due to the changes caused by the modification of the molecule orientation during the oxidation process. Independent Components Analysis (ICA), using the fast ICA algorithm, [22] has been used to facilitate the elucidation of the reaction mechanism. ICA is a data analysis technique that extracts the underlying source signals and their proportions from a set of mixed signals based on the assumption that these source signals are statistically independent.[22]

In this work, we have electrodeposited AuNPs by chronoamperometry on a single-walled carbon nanotubes (SWCNT) electrode. We have studied the SERS effect of AuNPs synthesized at different applied potentials and diverse deposition times. Optimal AuNPs have been used to study the adenine and guanine mechanism of oxidation. Thus, the main objective of this work is to obtain by Raman spectroelectrochemistry suitable information to explain simultaneously both, the oxidation mechanisms of purine bases, and the orientation of the intermediates that interact with the AuNPs electrodeposited on a press-transfer SWCNT electrode.

2. Material and methods

2.1. Reagents

SWCNT (Sigma-Aldrich), hydrogen tetrachloroaurate (III) hydrate, $HAuCl_4$. H_2O (Sigma-Aldrich), hydrogen chloride, KCl (Sigma-Aldrich), adenine (Sigma-Aldrich), guanine (Sigma-Aldrich) and potassium hydroxide, KOH (Lachema Neratovice) were used as received. All chemicals were analytical grade.

Aqueous solutions were prepared using high-quality water (NANOpure Diamond, Barnstead Nanopure, IMLAB).

2.2. Instrumentation

Electrochemical measurements were carried out at room temperature using a μAutolab III potentiostat. Raman spectra were obtained using a LabRAM HR Raman spectrometer (Horiba Jobin-Yvon). The samples were excited by He-Ne laser (633 nm) with a spectral resolution of approximately 1 cm^{-1}. A 50x objective was used and the laser power was approximately 1mW.

SEM imaging was performed using a high resolution SEM S-4800 (Hitachi).

A standard three-electrode cell was used in all experiments, consisting of a press transfer SWCNT electrode as working electrode, a Pt wire as auxiliary electrode and Ag/AgCl reference electrode. SWCNT electrodes were previously prepared using a methodology based on our previous work.[23] Briefly, 0.5 mg of SWCNT were dispersed in 100 mL of DCE, being the homogenization a fundamental step to obtain homogeneous films. Then, 0.8 mL of the SWCNT dispersion was filtered under vacuum using a hydrophilic teflon filter. Next the filtered film was dried at room temperature and using a laboratory hydraulic press, SWCNT film on the filter was transferred by pressure to a sheet of polyethylene terephthalate (PET) applying 25 ± 1 tons for 60 s. The separation of the filter was performed slowly and carefully using tweezers. The filter was pulled out with the tweezers so that the transfer of the SWCNT to the polymeric support provides a very homogeneous film with an area of 3.14 cm^2. The electrical contacts were made using conductive silver paint, creating a small line from the origin of the SWCNTs to the end of PET. Silver paint was dried in an oven and after further cooling, conductive silver paint was electrically isolated using insulating paint. Finally, the electrode was inserted into the oven at 75 °C for 120 minutes.

3. Results and Discussion

3.1. Optimization of AuNPs electrodeposition conditions.

AuNPs electrochemical deposition is usually performed by controlling either current[24] or potential.[25–31] Different techniques have been used in the electrosynthesis at controlled potential: linear voltammetry,[25,26] square wave voltammetry, simple pulse chronoamperometry,[29,30] double pulse chronoamperometry,[27,28] multi pulse chronoamperometry,[31] etc. In our case, chronoamperometry experiments have provided satisfactory results to obtain electrodes with SERS effect.

AuNPs electrodeposition on a SWCNT electrode was performed in a 5 mM $HAuCl_4$ and 0.5 M KCl solution to study the influence of potential and time. Once AuNPs were synthesized on the electrode, the Raman response of 1 mM adenine and KCl 0.01 M solution was analyzed. We considered adenine Raman spectrum recorded during 30 s as a reference to find optimum electrodeposition conditions. In particular we have chosen the most intense band of this molecule, the breathing Raman band (740 cm^{-1}), as response for this optimization. Fig.1.a shows the SERS effect of diverse substrates obtained at different potential for 100 s. When nanoparticles were deposited at 0.00 V, adenine bands were not observed, even breathing band was not present, indicating that suitable AuNPs to obtain a SERS response were not formed. At negative potentials (-0.75 V) breathing band began to evolve but the intensity was very weak. Maximum SERS intensity was observed when AuNPs were electrodeposited applying -1.25 V. In this case adenine breathing band was clearly differentiated and, therefore, it has been used to study the oxidation process of this molecule.

In the same way, deposition time is another important parameter to control in order to obtain the higher SERS effect. Fig.1.b shows an adenine Raman spectra applying -1.25 V at different electrodeposition times (20 s, 40 s, 60 s, 80 s, 100 s, 120 s). AuNPs

formed using an electrodeposition time of 20 s did not show SERS effect and in the Raman spectrum only the typical SWCNT bands were observed (Fig 1.b and Fig. S1). For an electrodeposition time of 40 s, a very weak breathing band of adenine was obtained. The signal improved significantly when the deposition time was increased to 60 s and a band centered at 740 cm^{-1} showed a much higher intensity than for shorter times. Raman signal showed the best response for 80 s deposition time, not only because the breathing band intensity was the highest but also because well-defined characteristic bands of different vibrational modes of adenine were observed, as for example 1380 and 1402 cm^{-1}. For longer electrodeposition times, Raman bands decreased their intensities and some bands disappeared. Therefore, from our experimental results, AuNPs synthesized on press-transfer SWCNT electrodes by applying -1.25 V for 80 s showed the best properties to obtain a good SERS effect for adenine (Fig 1.b and Fig. S1). AuNPs obtained by this methodology show spherical shape with a size around 40 nm (Fig. S2), but they tend to be agglomerated as is shown in Fig.2.

3.2. Adenine oxidation.

Different works have studied the orientation that adenine molecules adopt respect to metal surfaces. These works describe that adenine interacts in different modes depending on pH, concentration or metal (Au, Ag, Cu…) surface proposing three main binding modes: flat interaction (parallel),[32,33] end-on coordination (perpendicular)[34,35] and via the external amine group.[36] Raman spectroscopy is a very suitable technique to find out the orientation of the molecules and the combination of this spectroscopic technique with electrochemistry provides a whole view of the oxidation process.

Adenine oxidation was performed using a 1 mM adenine and 0.01 M KCl solution (pH = 5.85) by applying constant potentials between 0.00 V and +0.90 V and sampling each +0.10 V for 60 s to obtain each Raman spectrum.

ICA provides information of both the intermediates that are produced during the oxidation (Fig. S3.a) and the spectra (Fig. S3.b) of the initial adenine and the two different oxidation products. Adenine oxidation mechanism has been described in previous works[21,37,38]. These works suggest that adenine (A) is oxidized to 2-oxoadenine (2-oxoA) in the first oxidation step and 2,8-oxoadenine (2,8-dioxoA) is formed after the second oxidation process (Scheme 1). Cyclic voltammogram (Fig. S4) obtained by scanning the potential at 25 mV s^{-1} between 0.00 V and +0.90 V in a 1 mM adenine and 0.01 M KCl solution (pH = 5.85) does not show clear evidences of the two steps that take place in the adenine oxidation mechanism because the anodic peaks related to these processes are overlapped and only the second oxidation step is appreciated around +0.70 V. However, Raman spectroscopy is a suitable technique that provides *in-situ* spectroscopic information. In this case, although the electrochemical response does not provide clear information about the redox process, the spectroscopic signal yields molecular information that can be used to shed more light on the adenine oxidation mechanism.

Experimental and theoretical assignments of A, 2-oxoA and 2,8-dioxoA Raman bands has been proposed previously[39–44] from data experimentally obtained and from calculated data using density functional theory (DFT). The potential dependent SERS spectra of adenine adsorbed on AuNPs/SWCNT electrode, shown in Fig. 3, and the vibrational assignment, summarized in Table 1 are completely correlated to the adenine oxidation mechanism. Raman bands can be assigned to the different products generated

during the adenine oxidation by combination of these experimental and theoretical data with the ICA information.

At 0.00 V Raman spectra of adenine shows bands centered in 578 (wag C2-H), 630 (sqz C4-C5-C6, N1-C6-N10, C5-N7-C8), 737 (whole molecule ring breathing), 845 (str C5-N7), 945 (sqz N1-C2-N3), 962 (sqz N7-C8-N9), 1046 (sqz C4-N9-C8, str C5-N7), 1100 (bend C8-H, N10-H11, str C6-N10), 1345 (str C5-N7, N1-C2, bend C2-H, C8-H), 1380 (bend C2-H, C8-H, N9-H, str C6-N1, C8-N9, N3-C4), 1402 (bend N9-H, str C6-N10, N7-C8) and 1487 cm^{-1} (bend C8-H, str N7-C8). All the atoms of the adenine molecule are involved in these vibrations. Therefore, from this spectrum we conclude that at 0.00 V a parallel orientation of the adenine respect to the AuNPs surface is the most probable in our system. When the applied potential was increased to +0.40 V, adenine (A) is oxidized to form 2-oxoA, Scheme 1. Changes in different Raman bands are observed at this potential, some bands decrease their intensity (631, 737, 962, 1046, 1380 cm^{-1}) and others disappear (578, 945, 1100, 1487 cm^{-1}). This fact is related to the change in the orientation that indicates a lower participation of atoms N1, C2, N3, C4 and N9 because the molecule is slightly tilted (Fig. 5.a). Furthermore, Raman spectrum does not show the band of the C2-OH at 1020 cm^{-1}, confirming the orientation proposed. More changes were observed during the second oxidation process (at +0.70 V) when the 2-oxoA is oxidized to 2,8-dioxoA and the orientation is again modified (Scheme 1 and Fig. 5.a). Raman spectrum (Fig. 3) shows a new band centered in 1020 cm^{-1}, which is typical of the C-OH vibration.[45–47] The enolic form is more stable than the cetonic form due to the acid pH of the solution. The molecule 2,8-dioxoA acquires again a parallel orientation which explains that now the alcoholic band appears in the Raman spectra while it is not observed for the 2-oxoA. At potentials higher than +0.70

V the hydrolysis of 2,8-dioxoA takes place and Raman bands disappear, remaining only the bands characteristic of the electrode (AuNPs, SWCNT and PET).

3.3. Guanine oxidation.

Guanine oxidation was performed using a 1 mM guanine and 0.01 M KOH solution (pH = 13.1) by applying constant potentials between 0.00 V and +0.60 V and sampling each +0.10 V during 60 s to obtain each Raman spectrum. In this case, it was not necessary to reach as higher potentials as in the adenine oxidation because guanine oxidation takes place at a lower potential.[18]

Again, ICA provides information about the intermediates produced (Fig. S5) during the guanine oxidation process; there are two intermediates apart from the initial guanine.

Guanine oxidation mechanism has been also described in previous works[37,38,48]. The results presented in these works suggest that guanine (G) is oxidized to 8-oxoguanine (8-oxoG) in the first oxidation process and 8-oxoG loses two electrons to produce 8-oxoguanine oxidized (8-oxoG^{ox}) in the second oxidation step (Scheme 2). Cyclic voltammogram (Fig. S6) obtained by scanning the potential at 25 mV s^{-1} between 0.00 V and +0.60 V in a 1 mM guanine and 0.01 M KOH solution (pH = 13.1) does not show clearly the two anodic peaks related to the two oxidation steps that take place in the guanine oxidation mechanism. The anodic peaks of these processes are overlapped being appreciated a poor defined oxidation band around +0.30 V. As in the adenine case, Raman spectroelectrochemistry provides very useful spectroscopic information for a better understanding of the guanine oxidation mechanism.

Raman bands assignments of G, 8-oxoG and 8-oxoG^{ox} have been experimentally and theoretically (DFT) proposed. [43,44,49,50] Potential dependent SERS spectra of

guanine adsorbed on AuNPs/SWCNT electrode, shown in Fig. 4, and vibrational assignment, summarized in Table 2, are completely correlated to the guanine oxidation mechanism. Raman bands can be assigned to the different products generated during the guanine oxidation by combination of these experimental and theoretical data with the ICA information.

At 0.00 V Raman spectrum of guanine (G) shows bands centered in 533 (sqz C6-N1-C2, N3-C4-C5), 640 (whole molecule ring breathing), 738 (sqz N1-C2-N10, bend C6-O), 849 (bend C2-N3-C4, N1-C2-N3), 1032 (str N1-C6), 1166 (sqz N3-C4-C5), 1262 (bend N1-H, str C2-N10), 1312 (bend N1-H, N10-H12, str C2-N10, N3-C4), 1382 (bend N1-C2-N3), 1420 (str N1-C2, bend N1-H, rock NH_2) and 1718 cm^{-1} (str C6O-C5-C6, bend N1-H, sciss NH_2), these bands correspond to the vibrations in which atoms N1, C2, N3, C6 and N10 are involved. From these bands we conclude that the guanine orientation is perpendicular to the AuNPs surface at this potential, interacting through this part of the molecule with the AuNPs[51] as it is shown in Fig. 5.b. When guanine is oxidized to 8-oxoG at +0.10 V, Scheme 2, several Raman bands modify their intensity and position: bands centered in 533, 645, 738, 849, 1036, 1166, 1259, 1309, 1388, 1420 and 1718 cm^{-1} increase their intensity because more atoms (C4 and C5) are now interacting with the AuNPs and also a new band appears at 792 cm^{-1} (wag C4-C5-C6). The increment of these bands and, particularly, the evolution of the new band at 792 cm^{-1} band (out-plane) promote changes in the orientation and 8-oxoG starts to be slightly tilted (Fig. 5.b). At this orientation more atoms of the 8-oxoG are close to the AuNPs surface, so there are more or stronger interactions with AuNPs than in a complete perpendicular orientation: 533 (sqz N3-C4-C5), 849 (bend C5-N7-C8), 1166 (str C5-N7, sqz N3-C4-C5), 1312 (str C5-N7), 1382 (str C5-N7, bend N9-C4), 1420 (str C4-N9). However, the most important changes in Raman spectra are observed at +0.30 V.

During the second oxidation 8-oxoG loses two electrons to produce 8-oxoG^{ox}, Scheme 2. At this potential, 8-oxoG^{ox} changes completely the orientation respect to the 8-oxoG, being more tilted and acquiring a horizontal orientation parallel to the AuNPs surface. This change in the orientation is proved by the Raman spectra (Fig. 4): the evolution of new bands peaked at 332 (sqz N7-C5-C6, bend C6-O, C8-O), 415 (bend C6-O, C8-O, C2-N10), 493 (sqz C5-C6-N1, C2-N3-C4), 684 (bend C6-O, C8-O), 807 (bend C2-N3-C4, C5-N7-C8), 828 (sqz C4-N9-C8, str C5-N7), 932 (bend N3-C4-N9, N7-C5-C6, C5-N7-C8, str N7-C8) and 1130 cm^{-1} (str C5-N7, sqz N3-C4-C5) and the higher intensity of other bands 790 (bend N9-H, str N7-C8), 1434 (str N7-C8) and 1718 cm^{-1} (N7-C8O-N9) are related to all the atoms of 8-oxoG^{ox} that interact with the substrate, being the bands associated with the carbonyl groups proof of that. The vibration modes of carbonyl groups are observed in the Raman spectrum (332, 415, 684 and 1718 cm^{-1}) because the carbonyl group strongly interacts with the AuNPs and, in this parallel orientation, C6-O and C8-O groups are close to the AuNPs surface. At potentials higher than +0.40 V the 8-oxoG^{ox} hydrolysis takes places, the Raman bands related to the 8-oxoG^{ox} disappear and, finally, only the electrode bands are observed.

4. Conclusions

In the present work, the optimum conditions to electrosynthesize AuNPs by chronoamperometry with a strong SERS effect have been established. Different times and potentials have been used, with the maximum SERS response being obtained when a potential of -1.25 V was applied for 80 s. SEM characterization provided morphological information about the AuNPs deposited on a SWCNT electrode during the electrosynthesis process, showing that NPs tend to be agglomerated. The mechanism of oxidation of adenine and guanine has been elucidated analyzing the change in the

intensity and the shifting of the Raman bands of these compounds. Adenine shows a parallel orientation respect to the AuNPs surface at 0.00 V, when it is oxidized to 2-oxoA the molecule acquires a slightly tilted orientation, but after the second oxidation process to 2,8-dioxoA the molecule recovers the parallel orientation. In our conditions (pH, adenine concentration and AuNPs) the adenine does not adopt a perpendicular orientation, with a flat orientation being favoured. On the other hand, guanine orientation is perpendicular respect to the AuNPs surface at 0.00 V, but after the first oxidation at +0.10 V, 8-oxoG starts to be slightly tilted. The most important change in orientation is produced when the 8-oxoG is oxidized to 8-oxoG^{oxo} which acquires a parallel orientation respect to the AuNPs surface. Surface-enhanced Raman scattering at controlled potential has allowed us not only to characterize adenine and guanine oxidations, but also it has provided suitable information about the orientation of each intermediate.

Acknowledgments

The financial support made available by the Junta de Castilla y León (GR71, BU349-U13) and Ministerio de Economía y Competitividad (CTQ2010-17127) is gratefully acknowledged. D.I. thanks Ministerio de Economía y Competitividad for his predoctoral FPI fellowship. A.S. and M.K. acknowledge the support from MSMT ERC-CZ project: LL1301.

Supporting information

Further details of SEM images of AuNPs with the optimal electrodeposition conditions as well as Independent Components Analysis graphical representations of adenine and guanine oxidation mechanisms. This material is available free of charge via the Internet at http://pubs.acs.org.

References

(1) Fleischmann, M.; Hendra, P. J.; McQuillan, A. J. Raman Spectra of Pyridine Adsorbed at a Silver Electrode. *Chem. Phys. Lett.* **1974**, *26*, 163–166.

(2) Albrecht, M. G.; Creighton, J. A. Anomalously Intense Raman Spectra of Pyridine at a Silver Electrode. *J. Am. Chem. Soc.* **1976**, *99*, 5215–5217.

(3) Jeanmaire, D. L.; Van Duyne, R. P. Surface Raman Electrochemistry. Part 1. Heterocyclic, Aromatic and Aliphatic Amines Adsorbed on the Anodised Silver Electrode. *J. Electroanal. Chem.* **1977**, *84*, 1–20.

(4) Chourpa, I.; Lei, F. H.; Dubois, P.; Manfait, M.; Sockalingum, G. D. Intracellular Applications of Analytical SERS Spectroscopy and Multispectral Imaging. *Chem. Soc. Rev.* **2008**, *37*, 993–1000.

(5) Bantz, K. C.; Meyer, A. F.; Wittenberg, N. J.; Im, H.; Kurtuluş, O.; Lee, S. H.; Lindquist, N. C.; Oh, S.-H.; Haynes, C. L. Recent Progress in SERS Biosensing. *Phys. Chem. Chem. Phys.* **2011**, *13*, 11551–11567.

(6) Álvarez-Puebla, R. A.; Liz-Marzán, L. M. Environmental Applications of Plasmon Assisted Raman Scattering. *Energy Environ. Sci.* **2010**, *3*, 1011–1017.

(7) Tian, Z. Q.; Ren, B. Adsorption and Reaction at Electrochemical Interfaces as Probed by Surface-Enhanced Raman Spectroscopy. *Annu. Rev. Phys. Chem.* **2004**, *55*, 197–229.

(8) Kim, H.; Kosuda, K. M.; Van Duyne, R. P.; Stair, P. C. Resonance Raman and Surface- and Tip-Enhanced Raman Spectroscopy Methods to Study Solid Catalysts and Heterogeneous Catalytic Reactions. *Chem. Soc. Rev.* **2010**, *39*, 4820–4844.

(9) Lin, X. M.; Cui, Y.; Xu, Y. H.; Ren, B.; Tian, Z. Q. Surface-Enhanced Raman Spectroscopy: Substrate-Related Issues. *Anal. Bioanal. Chem.* **2009**, *394*, 1729–1745.

(10) Natan, M. J. Concluding Remarks: Surface Enhanced Raman Scattering. *Faraday Discuss.* **2006**, *132*, 321–328.

(11) Jana, N. R. Silver Coated Gold Nanoparticles as New Surface Enhanced Raman Substrate at Low Analyte Concentration. *Analyst* **2003**, *128*, 954–956.

(12) Muniz-Miranda, M.; Pergolese, B.; Bigotto, A.; Giusti, A. Stable and Efficient Silver Substrates for SERS Spectroscopy. *J. Colloid Interface Sci.* **2007**, *314*, 540–544.

(13) Guo, H.; Ding, L.; Mo, Y. Adsorption of 4-Mercaptopyridine onto Laser-Ablated Gold, Silver and Copper Oxide Films: A Comparative Surface-Enhanced Raman Scattering Investigation. *J. Mol. Struct.* **2011**, *991*, 103–107.

(14) Ibañez, D.; Fernandez-Blanco, C.; Heras, A.; Colina, A. Time-Resolved Study of the Surface-Enhanced Raman Scattering Effect of Silver Nanoparticles Generated in Voltammetry Experiments. *J. Phys. Chem. C* **2014**, *118*, 23426–23433.

(15) Cejkova, J.; Prokopec, V.; Brazdova, S.; Kokaislova, A.; Matejka, P.; Stepanek, F. Characterization of Copper SERS-Active Substrates Prepared by Electrochemical Deposition. *Appl. Surf. Sci.* **2009**, *255*, 7864–7870.

(16) Gao, P.; Gosztola, D.; Leung, L.-W. H.; Weaver, M. J. Surface-Enhanced Raman Scattering at Gold Electrodes : Dependence on Electrochemical Pretreatment

Conditions and Comparisons with Silver. *J. Electroanal. Chem.* **1987**, *233*, 211–222.

(17) Zhu, X.; Yang, H.; Wang, N.; Zhang, R.; Song, W.; Sun, Y.; Duan, G.; Ding, W.; Zhang, Z. A Facile Method for Preparation of Gold Nanoparticles with High SERS Efficiency in the Presence of Inositol Hexaphosphate. *J. Colloid Interface Sci.* **2010**, *342*, 571–574.

(18) Oliveira-Brett, A.; Piedade, J. A.; Silva, L.; Diculescu, V. Voltammetric Determination of All DNA Nucleotides. *Anal. Biochem.* **2004**, *332*, 321–3299.

(19) Paleček, E.; Bartošík, M. Electrochemistry of Nucleic Acids. *Chem. Rev.* **2012**, *112*, 3427–3481.

(20) Dryhurst, G. Electrochemical Determination of Adenine and Adenosine. *Talanta* **1972**, *19*, 768–778.

(21) Dryhurst, G. Dicarbonium Ions as Products of Electrochemical Oxidation of Biologically Important Purines at the Pyrolytic Graphite Electrode. *J. Electrochem. Soc.* **1969**, *116*, 1411–1412.

(22) Hyvärinen, A.; Oja, E. Independent Component Analysis: Algorithms and Applications. *Neural Networks* **2000**, *13*, 411–430.

(23) Garoz-Ruiz, J.; Palmero, S.; Ibañez, D.; Heras, A.; Colina, A. Press-Transfer Optically Transparent Electrodes Fabricated from Commercial Single-Walled Carbon Nanotubes. *Electrochem. Commun.* **2012**, *25*, 1–4.

(24) Reetz, M. T.; Helbig, W. Size-Selective Synthesis of Nanostructured Transition Metal Clusters. *J. Am. Chem. Soc.* **1994**, *116*, 7401–7402.

(25) El-Cheick, F. M.; Rashwan, F. A.; Mahmoud, H. A.; El-Rouby, M. Gold Nanoparticle-Modified Glassy Carbon Electrode for Electrochemical Investigation of Aliphatic Di-Carboxylic Acids in Aqueous Media. *Solid State Electrochem.* **2009**, *14*, 1425–1443.

(26) Huang, S.; Ma, H.; Zhang, X.; Yong, F.; Feng, X.; Pan, W.; Wang, X.; Wang, Y.; Chen, S. Electrochemical Synthesis of Gold Nanocrystals and Their 1D and 2D Organization. *J. Phys. Chem. B* **2005**, *109*, 19823–19830.

(27) Penner, R. M. Mesoscopic Metal Particles and Wires by Electrodeposition. *J. Phys. Chem. B* **2002**, *106*, 3339–3353.

(28) Liu, H.; Favier, F.; Ng, K.; Zach, M.; Penner, R. Size-Selective Electrodeposition of Meso-Scale Metal Particles: A General Method. *Electrochim. Acta* **2001**, *47*, 671–677.

(29) Wang, L.; Guo, S.; Hu, X.; Dong, S. Facile Electrochemical Approach to Fabricate Hierarchical Flowerlike Gold Microstructures: Electrodeposited Superhydrophobic Surface. *Electrochem. Commun.* **2008**, *10*, 95–99.

(30) Huang, C.; Jiang, J.; Lu, M.; Sun, L.; Meletis, E. I.; Hao, Y. Capturing Electrochemically Evolved Nanobubbles by Electroless Deposition. A Facile Route to the Synthesis of Hollow Nanoparticles. *Nano Lett.* **2009**, *9*, 4297–4301.

(31) Fernández-Blanco, C.; Colina, A.; Heras, A.; Ruiz, V.; López-Palacios, J. Multipulse Strategies for the Electrosynthesis of Gold Nanoparticles Studied by UV/Vis Spectroelectrochemistry. *Electrochem. Commun.* **2012**, *18*, 8–11.

(32) Suh, J. S.; Moskovits, M. Surface-Enhanced Raman Spectroscopy of Amino Acids and Nucleotide Bases Adsorbed on Silver. *J. Am. Chem. Soc.* **1986**, *108*, 4711–4718.

(33) Yamada, T.; Shirasaka, K.; Takano, A.; Kawai, M. Adsorption of Cytosine, Thymine, Guanine and Adenine on Cu(110) Studied by Infrared Reflection Absorption Spectroscopy. *Surf. Sci.* **2004**, *561*, 233–247.

(34) Watanabe, T.; Kawanami, O.; Katoh, H.; Honda, K.; Nishimura, Y.; Tsuboi, M. SERS Study of Molecular Adsorption: Some Nucleic Acid Bases on Ag Electrodes. *Surf. Sci.* **1985**, *158*, 341–351.

(35) Kundu, J.; Neumann, O.; Janesko, B. G.; Zhang, D.; Lal, S.; Barhoumi, A. Adenine and Adenosine Monophosphate (AMP) - Gold Binding Interactions Studied by Surface-Enhanced Raman and Infrared Spectroscopies. *J. Phys. Chem. C* **2009**, 113, 14390–14397.

(36) Ostblom, M.; Liedberg, B.; Demers, L. M.; Mirkin, C. A. On the Structure and Desorption Dynamics of DNA Bases Adsorbed on Gold: A Temperature-Programmed Study. *J. Phys. Chem. B* **2005**, *109*, 15150–15160.

(37) Oliveira-Brett, A. M.; Diculescu, V.; Piedade, J. A. P. Electrochemical Oxidation Mechanism of Guanine and Adenine Using a Glassy Carbon Microelectrode. *Bioelectrochemistry* **2002**, 55, 61–62.

(38) Brett, C. M. A.; Oliveira-Brett, A. M.; Serrano, S. H. P. On the Adsorption and Electrochemical Oxidation of DNA at Glassy Carbon Electrodes. *J. Electroanal. Chem.* **1994**, 366, 225–231.

(39) Li, J.; Fang, Y. An Investigation of the Surface Enhanced Raman Scattering (SERS) from a New Substrate of Silver-Modified Silver Electrode by Magnetron Sputtering. *Spectrochim. Acta. A. Mol. Biomol. Spectrosc.* **2007**, *66*, 994–1000.

(40) Huang, R.; Yang, H.-T.; Cui, L.; Wu, D.-Y.; Ren, B.; Tian, Z.-Q. Structural and Charge Sensitivity of Surface-Enhanced Raman Spectroscopy of Adenine on Silver Surface: A Quantum Chemical Study. *J. Phys. Chem. C* **2013**, *117*, 23730–23737.

(41) Giese, B.; McNaughton, D. Surface-Enhanced Raman Spectroscopic and Density Functional Theory Study of Adenine Adsorption to Silver Surfaces. *J. Phys. Chem. B* **2002**, *106*, 101–112.

(42) Lopes, R. P.; Valero, R.; Tomkinson, J.; Marques, M. P. M.; Batista de Carvalho, L. A. E. Applying Vibrational Spectroscopy to the Study of Nucleobases – Adenine as a Case-Study. *New J. Chem.* **2013**, *37*, 2691–2699.

(43) Castro, M.; Santamaria, R.; Charro, E.; Zacarias, A. Vibrational Spectra of Nucleic Acid Bases and Their Watson-Crick. *J. Comput. Chem.* **1999**, *20*, 511–530.

(44) D'Amico, F.; Cammisuli, F.; Addobbati, R.; Rizzardi, C.; Gessini, A.; Masciovecchio, C.; Rossi, B.; Pascolo, L. Oxidative Damage in DNA Bases Revealed by UV Resonant Raman Spectroscopy. *Analyst* **2015**, 140, 1477–1485.

(45) Li, D.; Li, D.-W.; Fossey, J. S.; Long, Y.-T. Portable Surface-Enhanced Raman Scattering Sensor for Rapid Detection of Aniline and Phenol Derivatives by on-Site Electrostatic Preconcentration. *Anal. Chem.* **2010**, *82*, 9299–9305.

(46) P. Neelakantan. The Raman Spectrum of Cyclohexanol. *Proc. Indian Acad. Sci.-Sect. A* **1963**, *57*, 94–102.

(47) Marley, N. A., Mann, C. K., Vickers, T. J. Determination of phenols in water using Raman spectroscopy. *Appl. Spectrosc.*, **1984**, *38* , 540–543.

(48) Li, Q.; Batchelor-McAuley, C.; Compton, R. G. Electrochemical Oxidation of Guanine: Electrode Reaction Mechanism and Tailoring Carbon Electrode Surfaces to Switch between Adsorptive and Diffusional Responses. *J. Phys. Chem. B* **2010**, 114, 7423–7428.

(49) Lopes, R. P.; Marques, M. P. M.; Valero, R.; Tomkinson, J.; De Carvalho, L. A. E. B. Guanine: A Combined Study Using Vibrational Spectroscopy and Theoretical Methods. *Spectrosc. An Int. J.* **2012**, 27, 273–292.

(50) Giese, B.; McNaughton, D. Density Functional Theoretical (DFT) and Surface-Enhanced Raman Spectroscopic Study of Guanine and Its Alkylated Derivatives. Part 1. *Phys. Chem. Chem. Phys.* **2002**, 4, 5161–5170.

(51) Jang, N. H. The Coordination Chemistry of DNA Nucleosides on Gold Nanoparticles as a Probe by SERS. *Bull. Korean Chem. Soc.* **2002**, *23*, 1790–1800.

Table 1: Vibrational assignment of adenine (A), 2-oxoadenine (2-oxoA) and 2,8-oxoadenine (2,8-dioxoA).[39–44]

Mode	A (0.00 V)	2-oxoA (+0.40 V)	2,8-dioxoA (+0.70 V)	Plane	Description
1	578	-	-	Out	Wag C2-H
2	630	631	635	In	Def R6 (sqz C4-C5-C6, N1-C6-N10), R5(sqz C5-N7-C8)
3	737	739	742	In	Whole molecule ring breathing
4	-	-	817	Out	Def R6(wag C4-C5-C6)
5	845	846	845	In	Def R5 (str C5-N7)
6	945	-	-	In	Def R6 (sqz N1-C2-N3)
7	962	965	962	In	Def R5 (sqz N7-C8-N9)
8	-	-	1020	In	Str C2-OH, C8-OH
9	1046	1046	1046	In	Def R5 (sqz C4-N9-C8, str C5-N7), R6 (sqz N1-C2-N3)
10	1100	-	-	In	Bend (C8-H, N10-H11), str (C4-N9, N3-C4, C6-N10)
11	-	1240	1257	In	Str C5-N7, N1-C2, C2-N3
12	-	1256	1255	In	Bend (C8-H, N9-H), str N7-C8
13	1345	1360	-	In	Str (C5-N7, N1-C2), bend (C2-H, C8-H)
14	1380	1388	1382	In	Bend (C2-H, C8-H, N9-H), str (C6-N1, C8-N9, N3-C4)
15	1402	1402	1420	In	Bend N9-H, str (C6-N10, N7-C8)
16	1487	-	-	In	Bend C8-H, str N7-C8

R5: five-membered ring; **R6:** six-membered ring; **bend:** bending; **def:** deformation; **rock:** rocking; **sciss:** scissoring; **sqz:** squeezing; **str:** stretching; **wag:** wagging

Table 2: Vibrational assignment of guanine (G), 8-oxoguanine (8-oxoG) and 8-oxoguanine oxidized (oxoGu^{ox}).[43,44,49,50]

Mode	G (0.00 V)	8-oxoG (+0.10 V)	8-oxoG^{ox} (+0.30 V)	Plane	Description
1	-	-	332	In	Def R5, R6 (sqz N7-C5-C6), bend C6-O, C8-O
2	-	-	415	In	Bend C6-O, C8-O, C2-N10
3	-	-	493	In	Def R6 (sqz C5-C6-N1, C2-N3-C4)
4	533	533	528	In	Def R6 (sqz C6-N1-C2, N3-C4-C5)
5	640	645	645	In	Whole molecule ring breathing
6			684	In	Bend C6-O, C8-O
7	738	738	735	In	Def R6 (sqz N1-C2-N10), bend C6-O
8	-	792	790	Out	Def R6 (wag C4-C5-C6), R5 (tors N7-C8)
9	-	-	807	Out	Bend C2-N3-C4, C5-N7-C8
10	-	-	828	In	Def R5 (sqz C4-N9-C8, str C5-N7)
11	849	849	849	In	Bend (C2-N3-C4, C5-N7-C8, N1-C2-N3)
12	-	-	932	Out	Bend N3-C4-N9, N7-C5-C6, C5-N7-C8), str N7-C8
13	1032	1036	1018	In	Str (C8-N9, N1-C6), bend N9-H
14	-	-	1129	In	Str (C5-N7), def R6 (sqz N3-C4-C5)
15	1166	1166	1174	In	Str C5-N7, def R6 (sqz N3-C4-C5)
16	1262	1259	1259	In	Bend N1-H, N9-H, str (C2-N10, N7-C8)
17	1312	1309	1309	In	Bend (N1-H, N10-H12), str (C5-N7, C2-N10, N3-C4)
18	1382	1388	1376	In	Str C5-N7, bend (N1-C2-N3, N9-C4)
19	1420	1420	1434	In	Str (N1-C2, N7-C8, C4-N9), bend N1-H, rock NH2
20	1718	1718	1718	In	Str (C6O-C5-C6, N7-C8O-N9), bend N1-H, sciss NH2.

Schemes

Scheme 1. Adenine oxidation mechanism

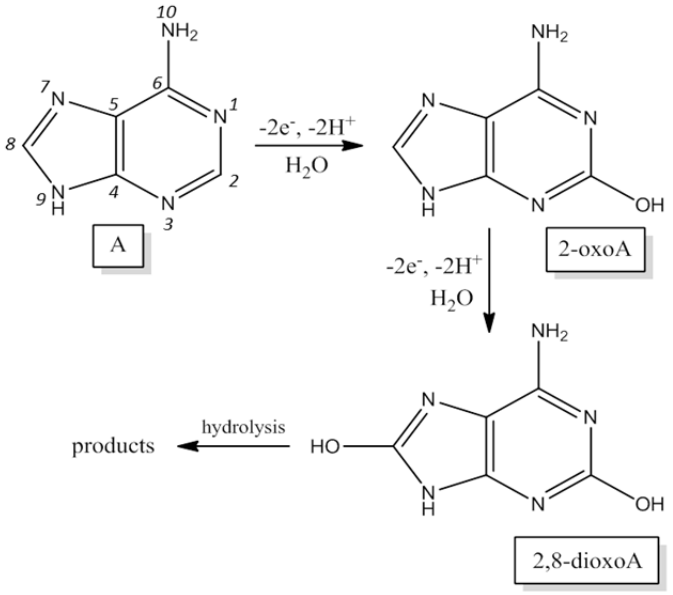

Scheme 2. Guanine oxidation mechanism.

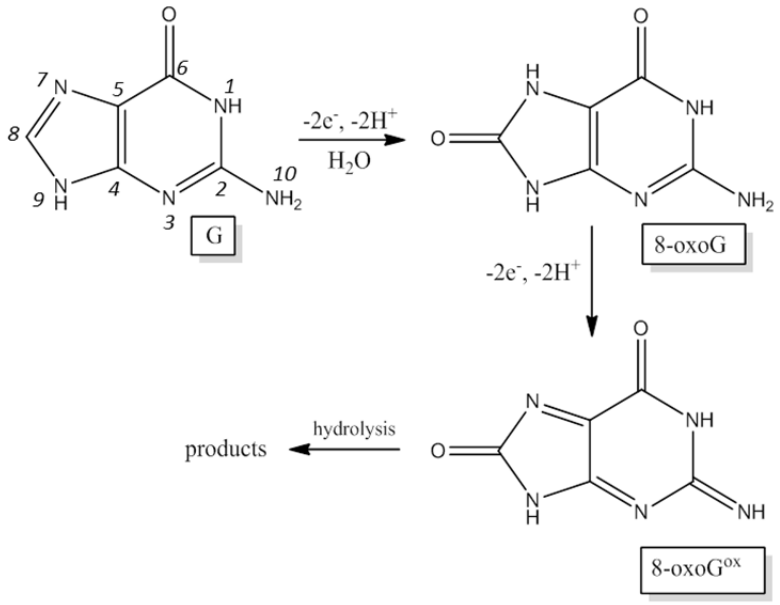

Figures

Figure 1.a

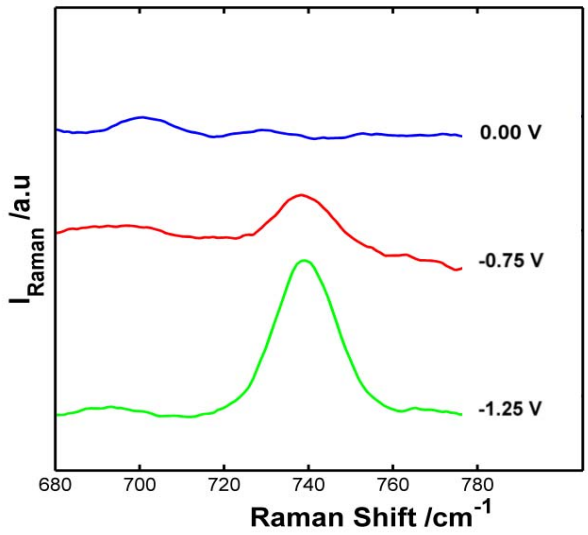

Figure 1.b

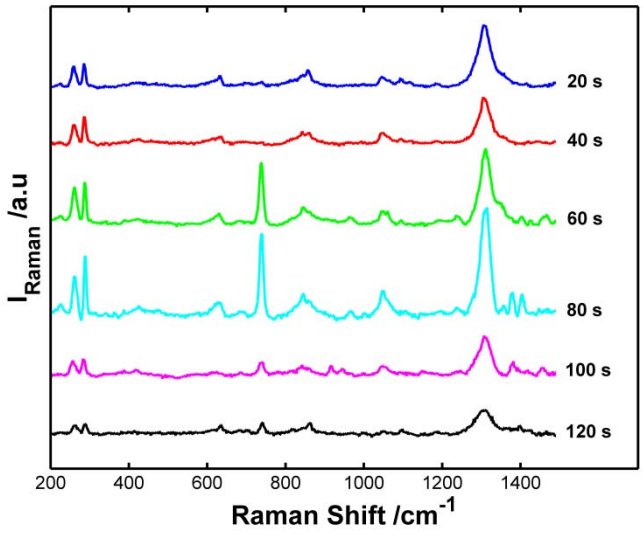

Figure 1. Raman spectra of adenine at different potentials (a) and times (b) of AuNPs electrodeposition.

Figure 2

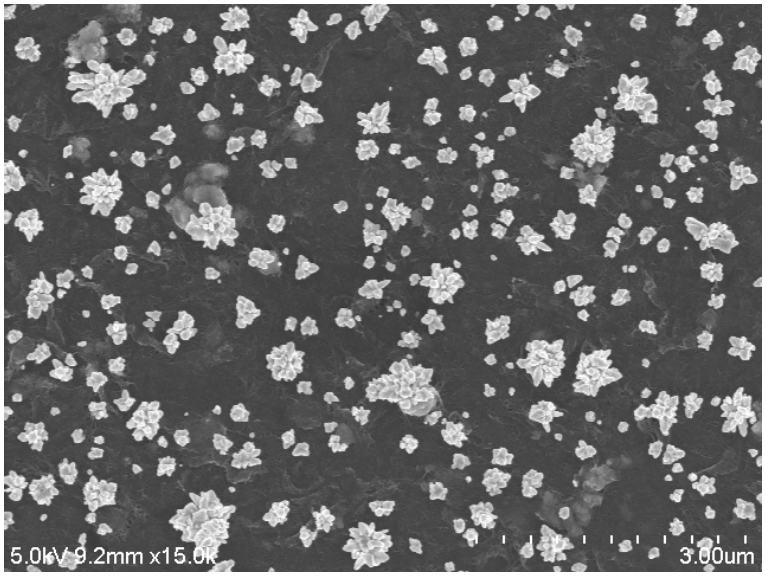

Figure 2. SEM image of AuNPs synthesized using the optimum electrodeposition conditions.

Figure 3

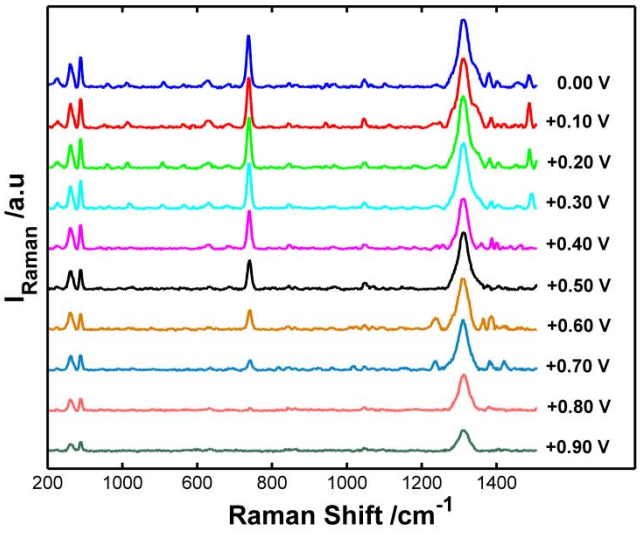

Figure 3. Evolution of the Raman spectra of adenine at different electrode potentials.

Figure 4

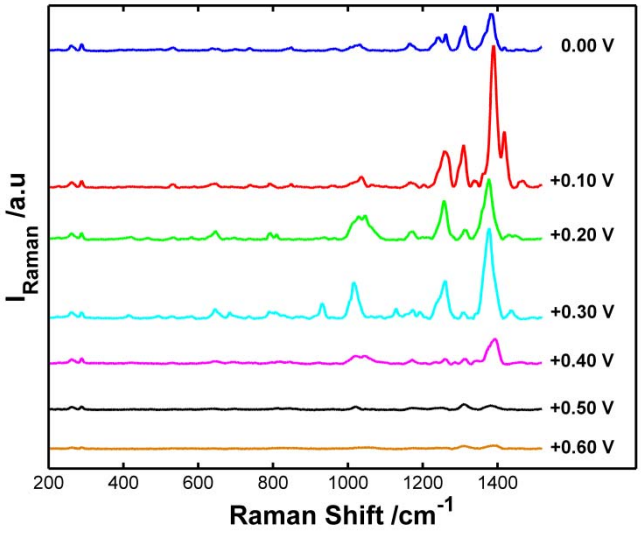

Figure 4. Evolution of the Raman spectra of guanine at different electrode potentials.

Figure 5

Figure 5.a

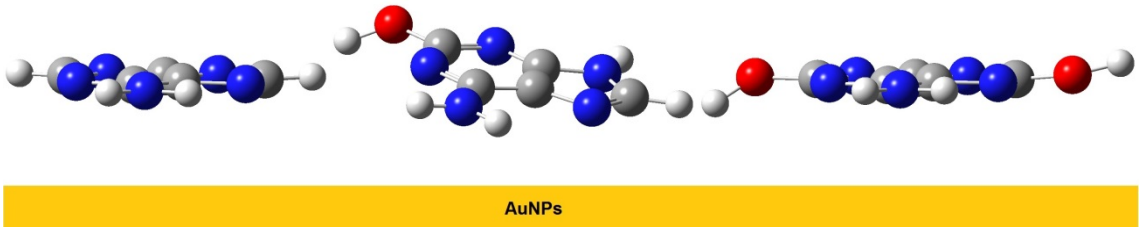

Figure 5.b

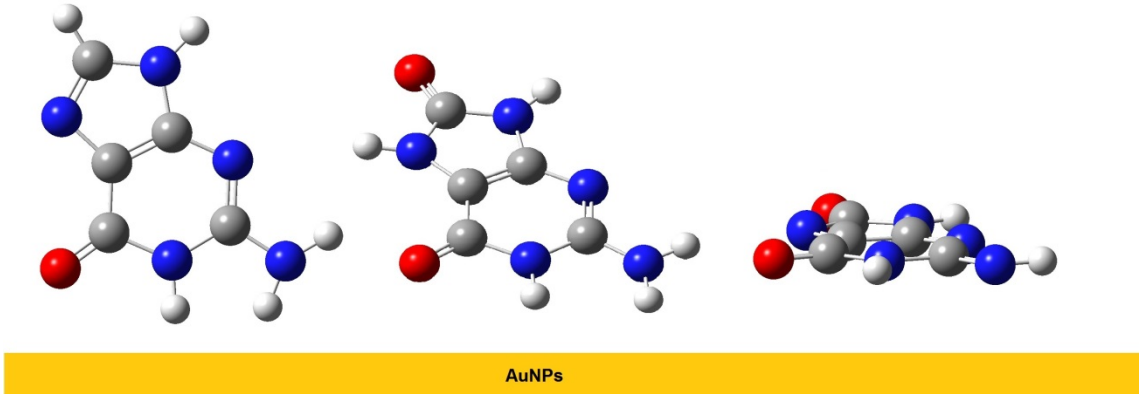

Figure 5. Schematic drawing of (a) A, 2-oxoA and 2,8-dioxoA orientation during the oxidation and (b) G, 8-oxoG and 8-oxoG^{oxo} oxidized orientation during the oxidation.

Table of contents (TOC)